Hypersonics: laying the road ahead

Pedro Gonçalves
pedro.simoes.goncalves@tecnico.ulisboa.pt

Instituto Superior Técnico, Lisboa, Portugal

May 2018

Abstract

This work provides a technology roadmap for hypersonic applications and use it to some extent in preliminary hypersonic aircraft design. A survey on barriers preventing hypersonic flight was conducted and a technology roadmap was created based on novel concepts which could address the critical requirements. Three engines (ramjet, scramjet and rocket) were numerically modeled in SUAVE, a framework tool developed by Embraer and Stanford University, to run low-fidelity hypersonic vehicle analysis. Since the tool lacked a detailed hypersonic background, simple aerothermodynamic and weight distribution capabilities were also added. These new models were compared against numerical codes and/or experimental data for validation before being implemented in SSTO and atmospheric cruise mission scenarios that assessed the usefulness of new technologies and the performance of its subcomponents. With this work, a new proposal for the future of hypersonics is presented and SUAVE is now able to run basic hypersonic simulations;

Keywords: Hypersonic, Roadmap, Technology, Low-fidelity

1. Introduction

Imagine traveling from London to Sydney in less than four hours. Imagine a regular round-trip flight aboard a commercial spaceplane to a space hotel in Low Earth Orbit (LEO) for an affordable price. More than half a century after the technological marvels that put Mankind on the Moon, these two concepts still seem somewhat eccentric and share a common notion of uncertainty. As of March 2018, a flight from London to Sydney doesn't take less than 17 hours (all-time record); on the other hand, the only handful of space tourists who have visited and stayed at the International Space Station since the turn of the century have paid no less than $20,000,000 (2018) for their journey, far from affordable. However, all of these projects may become a reality if sustainable hypersonic capabilities are provided.

Hypersonic flight is the next major leap forward in aerospace and despite not being an entirely new concept, it has been gathering more attention from the scientific community in recent years. The ability to significantly cut travel times and bring cities, nations and people even closer will revolutionize and strengthen interpersonal and economical ties, as well as redefine the notion of distance: traveling to the opposite side of the world by plane could take almost the same time as a roadtrip across the entire extent of continental Portugal. Rightfully so, this justifies the research and development of new technologies to enable sustainable and affordable hypersonic transport. The implications of a successful hypersonic program are significant, not only for terrestrial applications but also for routine space access, a goal that dates back almost 60 years and is yet to be accomplished. Not only hypersonics can connect people all over the planet, it can become a bridge towards Space exploration and colonization by lowering costs associated with Space endeavors.

Mastering hypersonics is a complex challenge and while this work cannot, in any way, achieve such an encompassing level, it serves as a starting point to tackle the many intricacies of hypersonic flight; this includes understanding current technological barriers and gaps, map new enabling technologies with the potential of unlocking hypersonic capabilities and apply them in a preliminary design analysis tool, SUAVE, to better understand how they may impact overall aircraft performance.

2. Background

2.1. Roadmap requirements

Before beginning to map enabling technologies in the field of hypersonics, a roadmapping structure and strategy are required.

A technology roadmap is a tool to support strategic and long-range planning by matching both short and long term goals to specific technological solutions. For the purpose of this work, the roadmap structure used is adapted from the Defense Logistics Agency of the United States Department of Defense [2].

To evaluate each technology, a scale is required to provide a universal comparison method. Among other scales, the technology readiness level (TRL) was selected as a reference scale for this project. By using a standard TRL, the common assessment of individual technologies allows for risk reduction both in budget and planning processes. For the purpose of this work, the same TRL standard as that of the European Space Agency for Space product development is used [1], presented in Figure 1.

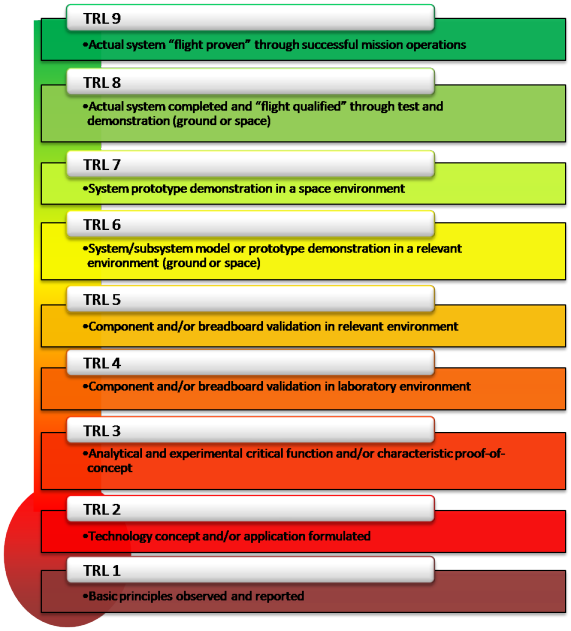

Figure 1: TRL scale [1]

2.2. State of the art

Understanding hypersonic state-of-the-art is paramount to the success of this work. By doing so, it is possible not only to list hypersonic concepts and technologies that have already been demonstrated, but also to comprehend the technological barriers preventing an extensive hypersonic application.

Sonic boom Currently there are no industry standards for the acceptability of a sonic boom and the overground ban of supersonic commercial travel from the 1970s still endures. NASA is currently experiencing with design innovations such as boom shaping for the Quiet Supersonic Technology demonstrator (QueSST), with the goal of reassessing current regulations and providing a quieter alternative for supersonic transport [15].

Aerodynamics One of the most promising concepts in hypersonic aerodynamics is the waverider configuration which makes use of shock waves being generated by the airframe to act as lifting surface, in a phenomenon known as compression lift. The Boeing X-51 is the latest vehicle known to have demonstrated such capability, in 2013. However, despite its success, there are major technological issues preventing a wider application. Scaling this concept to the size of commercial airliners or spacecraft is currently unfeasible as a result of the very low volumetric efficiency of the waverider concept. Another problem is that this design only works for a particular Mach number, resulting in a significant reduced lift capability when operating in off-design conditions.

Propulsion There are severe limitations in current propulsion systems that render sustained air-breathing hypersonic flight unachievable. Air-breathing engines outperform conventional rockets in regards to specific impulse, safety and maneuverability. However, they are substantially harder to design and test.

Conventional turbojet engines cannot single-handedly propel an aircraft to Mach 3+. On the other hand, supersonic and hypersonic propulsion concepts such as ramjets and scramjets are only now becoming feasible but they require supersonic speeds to be ignited. As a result, they are useless during the subsonic portion of flight. If a spaceplane is envisioned, rocket engines must be incorporated into the propulsion system for orbital assist. However, because oxidizer has to be carried on-board, there is a significant payload weight penalty. This penalty is, in fact, so substantial that current rocket engines cannot carry enough propellant efficiently in a single stage to reach orbit; this drives the costs up as multiple stages are required. The most recent take on this issue is SpaceX's concept of reusable first-stage engines.

The most powerful, proven, reusable high-speed air-breathing engine conceived to date is the Pratt & Whitney J58, which powered the Lockheed SR-71 "Blackbird" up to Mach 3 with technology developed 60 years ago. This could only be possible with a high bypass afterburner at a very high fuel burn rate, effectively making it a turbo-ramjet engine.

Materials Regarding airframe and other aircraft external structures, sustained hypersonic flight is strongly limited by the materials used. To survive the harsh hypersonic conditions, they must be strong enough to withstand high heat fluxes, temperatures and temperature gradients. They must also provide shielding against oxidation and erosion while supporting strong aerodynamic loads. Critical conditions take place on the vehicle nose and wing leading edge. Temperature requirements on a sharp leading edge for a cruise hypersonic vehicle are in the order of 2000 to 3000°C, substantially

higher when compared with the reinforced carbon-carbon used in the Space Shuttle orbiter.

TPS Thermal protection systems (TPS) incorporate different technologies that help the vehicle resist excess heat in hypersonic flight. They are not only dependent on the material properties but other mechanisms that can be implemented to alleviate thermal loads. State-of-the-art TPS has been applied to re-entry spacecraft. When it comes to reusable concepts, the Space Shuttle TPS, composed of TUFI ceramic tiles, could sustain multiple re-entries at up to 100 W/cm^2[17]. However, upon landing, panels would require significant maintenance, resulting in high turnaround times and repair costs. Ultimately, mechanical failure (i.e., very low impact resistance) was the main reason behind the fatal Challenger disaster, showing how susceptible the system was to mechanical anomalies.

GNC One of the biggest accomplishments in Guidance, Navigation and Control (GNC) systems dates back to the 80s, when then the Soviet Union managed to launch and land Buran, a fully automatic spaceplane. This was an extraordinary feat considering how rudimentary GNC theory and technology was back in this age. Buran was the first space shuttle to perform an unmanned flight and still holds the record of the largest aircraft to orbit and land unmanned [3]. Recently, there has been progress in the hypersonic GNC field, such as demonstrations for the Boeing X-51 scramjet-powered aircraft. Nevertheless, one of the most advanced GNC systems of today must be that of the Boeing X-37. This secretive spaceplane is taken to LEO through expendable rocket engines, where it then conducts its classified missions before performing a fully autonomous re-entry and landing

2.3. Novel concepts

To fill in the gaps from the current state-of-the-art, a survey of enabling technologies was conducted. The most promising concepts were listed and described with a moderate level of detail to provide a basic overview of their functionality. Table 1 sorts them by technological area and associates them to a TRL.

2.4. Roadmap implementation

Upon reviewing some of the most significant technological prospects for hypersonic applications, the next step in the roadmapping procedure is to select the best alternatives to fill in the requirements. This recommendation is based on the current TRL, the current R&D efforts towards its completion and expected timeline for delivery. To do so, data on projected timelines for TRL 8 was collected based on manufacturer/developer references. These were corrected based on personal interpretation, taking into account how old the references were and what progress has been recently achieved for each technology. All this information is compiled in the final technology roadmap timeline displayed in Figure 2.

Area	Technology	TRL
Propulsion	High-speed turbine	6
	Dual-mode scramjet	7
	Continuous Rotating Detonation	4
	Rocket-based combined cycle	3-4
	Turbine-based combined cycle	5-6
	Turbine-rocket based combined cycle	2-3
	Magneto-hyodrodynamic drive	3
	SABRE	3
	Scimitar	3
	Pre-cooled turbojet	4-5
Material	Ultra-high temperature ceramics	4-5
	Ceramic Matrix Composites	7
	Metallic Matrix Composites	7
	Polymer nanocomposites	3-4
	Boron nitride nanocomposites	4
	Reinforced Carbon Carbon	9
TPS	High-performance heat pipe	6
	Electron transpiration cooling	2
	Structurally Integrated TPS	3-4
	TUFROC	9
	Opacified Fibrous Insulation	4
	Internal Multi-screen Insulation	4
Aerodynamics	Hypersonic I-plane aircraft configuration	1-2
	Distributed roughness	3
Sonic mitigation	Configuration shaping	1-2
	Plasma boom optimization	2-3

Table 1: Novel concepts and respective TRL

3. Implementation

3.1. Test case

After concluding the technology roadmap and identifying high-potential technologies for hypersonic applications, the goal is to create a numerical model for some of those technologies in SUAVE, a framework tool developed by Embraer and Stanford University, which currently has no hypersonic capabilities. By doing so, it is possible to assess the impact of novel technologies in determining the minimum requirements to transport a specified payload. Since the main focus of this analysis is placed in the individual performance of hypersonic technologies, there is a need for a vehicle-oriented assessment rather than mission-oriented. To provide a more robust analysis, the same vehicle is applied to two different test cases, facing distinct conditions: an hypersonic cruise vehicle and an ascent-and-reentry vehicle.

A small hypersonic aircraft is envisioned, hereby referenced as Hypersonic Multi-purpose Vehicle (HMV). Both the air-breathing cruise and the ascent-and-reentry variations (hereby referenced as HMV-CAV and HMV-ARV, respectively) share the exact same design. For its initial sizing, the Lockheed SR-72 was used as a baseline.

Despite being designed to fulfill the same goal, HMV-CAV and HMV-ARV operate in very different regimes given the clear distinction in freestream

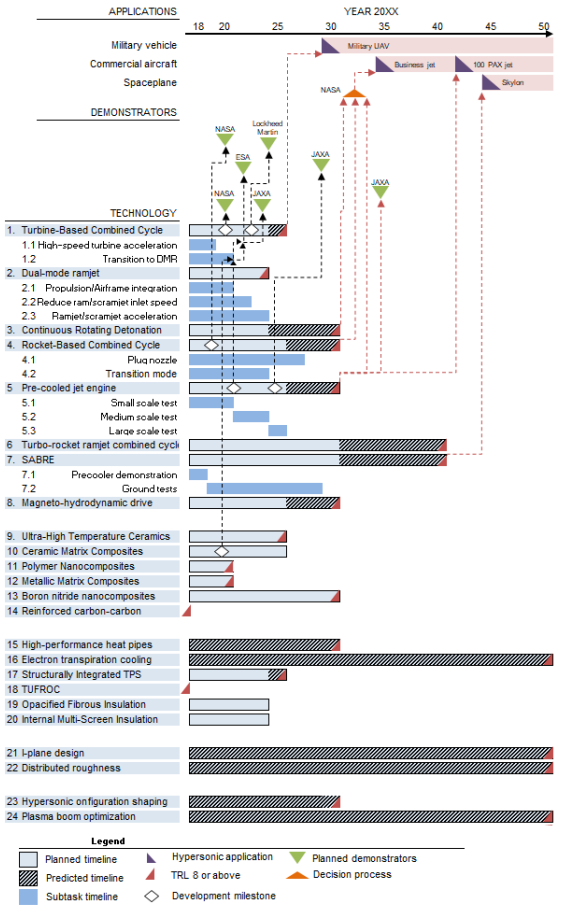

Figure 2: Proposed roadmap

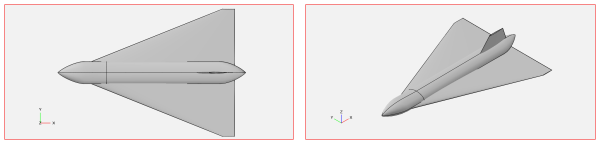

(a) Top view (b) Isotropic perspective

Figure 3: HMV final design

conditions each vehicle faces.

For the case of the HMV-CAV, it has an apparently similar mission profile to that of a regular subsonic airliner. However, the climb segment is usually done at constant dynamic pressure to avoid excessive loads on the vehicle structure during this high-speed maneuver

For the HMV-ARV, the spacecraft will follow a similar trajectory to that of the HMV-CAV during the initial climb phase, at constant dynamic pressure. Upon reaching a sufficiently high Mach number and altitude, air-breathing operation is shut down and the rocket engine kicks in; this marks the beginning of a final ascent phase up until maximum altitude is reached. From here, the re-entry phase takes place.

Upon reviewing the roadmap and analyzing the predicted mission profiles, it was decided the best engines to model for each test case would be a turbine-based combined cycle (HMV-CAV) and a turbine-rocket based combined cycle (HMV-ARV).

3.2. Numerical models

SUAVE does not incorporate any numerical methods targeting hypersonic flight in particular. Current supersonic capabilities extend to propulsion and aerodynamic correlations based on empirical or semi-empirical laws. Therefore, after analyzing the actual SUAVE capabilities and cross-checking them with the basic requirements to run the academic test case, a number of numerical methods were labeled as necessary to perform a basic hypersonic analysis.

Weight distribution Hypersonic aircrafts require complementary structures that enable them to fly at such speeds (e.g., TPS, cryogenic storage tanks, structural reinforcements). As such, the empirical relations currently used for subsonic aircraft design might fail to correctly estimate its weight. SUAVE has several different methods for aircraft weight estimation depending on airframe design (i.e., tube and wing, blended wing body), even accounting for out-of-the-ordinary propulsion systems (i.e., human and solar-powered). Because none of them fit the test case requirements, the Hypersonic Aerospace Sizing Analysis (HASA) weight estimation method was used [12].

LOX/LH2 rocket engine To design a low-fidelity model for preliminary rocket performance, the ideal rocket theory [9, 20] is applied, which predicts that specific impulse is a function of a drag coefficient, C_D and thrust coefficient, C_F.

$$I_{sp} = \frac{C_F}{C_D \cdot g} \tag{1}$$

Given the complex relations between variables, a single model for liquid rocket propulsion was created using exclusively a propellant combination of LOX and LH2. Combustion parameters are set based on Braeuning [6]: using the plots of adiabatic flame temperature, gas molecular weight and specific heat ratio with respect to chamber pressure and O/F, polynomial and logarithmic functions were built using EXCEL and used for interpolation.

To verify the numerical model, data on several LOX/LH2 engines was collected [7, 23, 10, 11]. The sample is wide and diverse, contemplating engines from different decades purposefully built with distinct on-design conditions (i.e.g, RD-0120 is a first-

stage engine whereas Vulcain 2 is a second-stage engine). The next step was to use information compiled from Braeuning to calculate specific propellant properties and obtain values for specific impulse, which were then compared to experimental data on each engine, both at sea level (if applicable) and vacuum. Figure 4 provides a visual representation of the validation process for all engines, including the parameters used in the calculations.

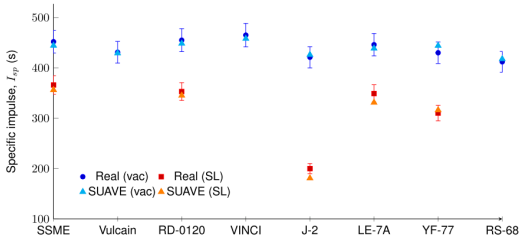

Figure 4: LOX/LH2 rocket engine model validation, error bars of 5%

Ramjet The ramjet model was expanded upon the existing turbojet model available in SUAVE. New constraints were added (e.g., thermal choking) and underlining simplifications were assumed. For instance, the flow is considered steady, quasi-one dimensional, purely axial and behaves as perfect gas. The engine is comprised of a diffuser, burner and exit nozzle, a seen in Figure 5.

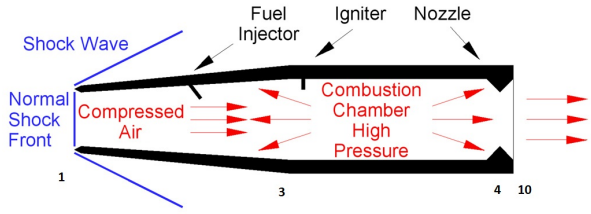

Figure 5: Ramjet engine schematics [13]

For the purpose of this demonstration, a simple diffuser design is implemented, using only one normal shock to decelerate the flow. This initial approach is much less efficient and results in a conservative estimate for the diffuser performance. Using Rayleigh flow equations, there is a cap on the heat transfer to the flow in the combustion chamber. This translates to a maximum exit temperature related to thermal choking, T_R. There are also temperature restrictions related to the materials used downstream of the burner; for turbojets, this is a high pressure turbine, where mechanical and thermal stresses are very high due to rotation; for a ramjet engine, this is the nozzle chamber, which withstands much higher temperatures. Finally, the flow exits through the expansion nozzle, where it is considered to be fully expanded.

The new SUAVE ramjet model is verified with theoretical quasi-one dimensional performance predictions of specific impulse. Firstly, a range of I_{sp} for ramjet engines was obtained for hydrocarbon and hydrogen fuels. Then, general SUAVE efficiencies were set, the same for both fuel types. These values ranged from 95 to 100% to move away from the ideal ramjet performance. To compare the numerical model with the expect I_{sp} range, JP-7 and LH2 were chosen for the simulation; that is, data on the fuel combustion heat, stoichiometric fuel-to-air ratio and energy density was collected [22, 8].

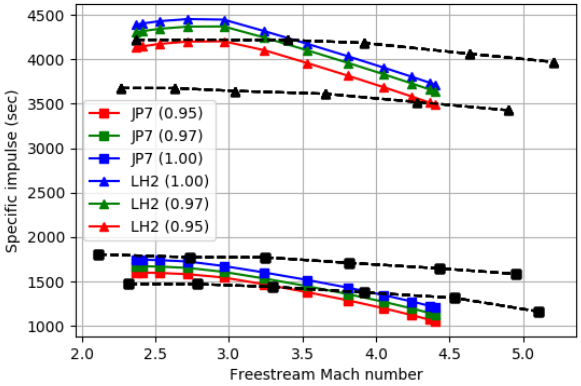

Figure 6: Ramjet model verification

Scramjet To design a low-fidelity model of scramjet engine, core assumptions were considered to reduce the number of constraints to the problem. The Heiser and Pratt methodology [14] was applied; this implies the use of cycle static temperature ratio to model the inlet, a constant-pressure combustion with a fixed stoichiometric fuel-to-air ratio in the burner and a fully expanded flow in the nozzle.

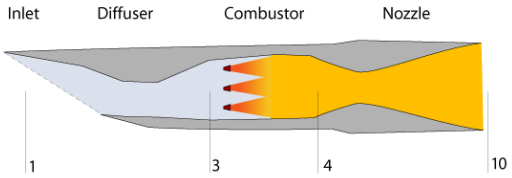

Figure 7: Scramjet engine schematics [19]

Since scramjet technology is still an active, high-priority research topic, there is a lack of publicly available experimental data to validate this model. There are, nonetheless, numerous scramjet numerical models available. For the verification process, three different scramjet codes were used: Ramjet Performance Analysis Code (RJPA), Simulated Combined-Cycle Rocket Engine Analysis

Module (SSCREAM) and VTMODEL. The verification process used liquid hydrogen as fuel with stoichiometric fuel-to-air-ratio. The SUAVE model parameters and the numerical model comparison can be consulted in Figure 8.

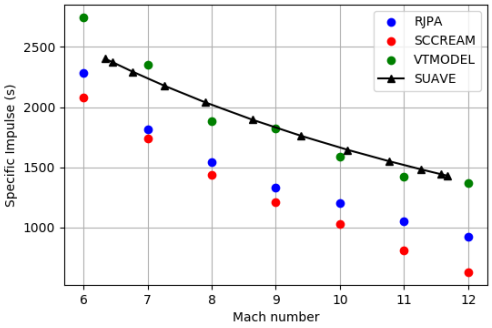

Figure 8: Scramjet model verification

Most of the combustion-related parameters were assumed from Heiser and Pratt [14] as they have no equivalent to any of the codes used for comparison. The results highlight some of the discrepancies that exist between other numerical models and demonstrate the scramjet sensibility to minor modifications in flow properties and component efficiency. Nevertheless, the newly implemented SUAVE scramjet model provides a specific impulse estimate either within the expected range or with a small deviation from it, which is sufficient for a preliminary design basis.

Aerothermodynamic and re-entry model There are several aerothermodynamic models that help predict temperatures and heat fluxes across all sections of an airframe. Higher-fidelity models rely on CFD software but are unnecessarily computational-heavy for preliminary design. For a simpler approach, the aerothermodynamic analysis in SUAVE will be performed based on semi-empirical laws. Perhaps the simplest method for estimating hypersonic aerodynamic heating is to use Equation 2, an approximation for trans-atmospheric vehicles derived from Anderson [16]

$$q_w = {\rho_\infty}^{0.5} \cdot {V_0}^3 \cdot 1.83 \times 10^{-8} \cdot {r_{LE}}^{-1/2} \tag{2}$$

$$Q_W = \int_{t=0}^{t=t_f} q_w dt \tag{3}$$

In SUAVE, mission profiles are built from different segments, properly arranged in climb, cruise, hover or descent categories. For atmospheric operations there are plenty of mission segments to choose from but there are none available for spacecraft trajectories, including re-entry. For the HMV-ARV, it is necessary to create such segments to study heat flux distribution during re-entry. For maximizing the spacecraft range, a lifting trajectory model is chosen. In a lifting reentry, there are four main forces being exerted on the aircraft: weight, drag, lift and centripetal force. Equations for velocity and acceleration throughout re-entry are listed below:

$$v = v_{re} \cdot \left[1 + \frac{\rho_o R_{Earth}}{2\beta} \frac{L}{D} e^{-h/h_s}\right]^{-\frac{1}{2}} \tag{4}$$

$$n = -\frac{1}{\frac{2\beta}{\rho_o R_{Earth}} e^{h/h_s} + \frac{L}{D}} \tag{5}$$

The IXV spacecraft was used as reference to validate both the atmospheric re-entry and the aerothermodynamic model and to do so requires vehicle and trajectory information [5]. The final results of the validation process are displayed in Figure 9. The reentry profile matches the actual flight data (expected re-entry time of $\approx$ 20 minutes) and the maximum experimental heat flux is of 65 W/cm^2, which corresponds to a 4.6% relative error for a $C_D = 0.4$.

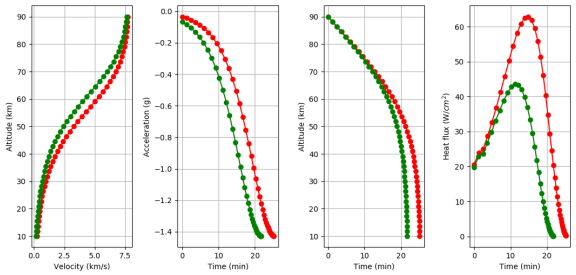

Figure 9: Atmospheric and aerothermodynamic model validation, for $C_D = 0.4$ (red) and $C_D = 0.7$ (green)

4. Results

Results for the HMV-CAV and HMV-ARV are presented below.

4.1. Air-breathing cruise (HMV-CAV)

Mission profile selection For a hypersonic air-breathing cruise and acceleration vehicle, climb is done at constant dynamic pressure. When this parameter is fixed, the cruise altitude (influenced by the freestream density) automatically determines the cruise speed. On the other hand, for hypersonic flight, the cruise Mach number must be at least higher than 4.0. Therefore, there is range of values for dynamic pressure (between 25 and 80 KPa)

and cruise altitude (between 20 and 25 km) that fulfill all the requirements.

From a performance standpoint, there is a general interest in reducing the flight duration but also maximizing the flight range, with a fixed amount of fuel. The optimum cruise design point is therefore chosen based on the best trade-off between these two variables, represented by the utility function, U, shown in Equation 6. For each coordinate (q, h), the values for the maximum and minimum range and duration are stored and the cruise distance is iteratively increased until a final fuel margin of $(2.50 \pm 0.30)\%$ is reached. For each pair (q, h), U returns a value from 0 to 1, where 1 is the best possible result and 0 is the least favorable. The function is plotted in Figure 10 for 225 coordinates. The final climb design conditions are set to 45 KPa and 25 km.

$$U(q,h) = \frac{1}{2} \cdot \frac{X - X_{min}}{X_{max} - X_{min}} + \frac{1}{2} \cdot \left(1 - \frac{t - t_{min}}{t_{max} - t_{min}}\right) \tag{6}$$

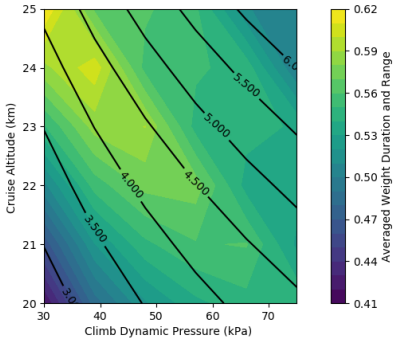

Figure 10: HMV-CAV utility function. Contour lines represent cruise Mach number, M

Baseline solution The final mission profile is displayed in Figure 11. The heat flux distribution at the stagnation point of the vehicle nose is demonstrated in the left graph of Figure 13. This point in particular is chosen as it undergoes some of the most severe heating conditions. In the right graph of Figure 13, L/D is plotted over time; the red-dashed line represents the Kuchemann empirical relation [4] for L/D_{max} in hypersonic flight. Figure 12 displays the thrust at all points of the mission and the throttle value that was iterated to provide said thrust. From this figure, throttle exceeds 100% in certain mission segments which indicates that the engine is not sized correctly; that is, it's producing a higher thrust than what it is capable of. This calls for a corrected solution.

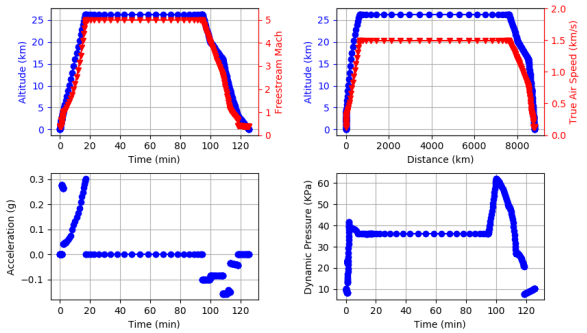

Figure 11: HMV-CAV mission profile

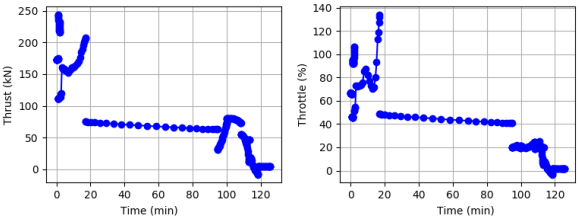

Figure 12: HMV-CAV propulsion general parameters

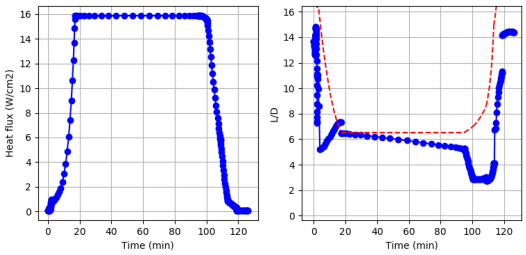

Figure 13: HMV-CAV aerothermodynamic and aerodynamic analysis

Enhanced solution As mentioned above, while in general the results obtained for the baseline solution are satisfactory, there is a misrepresentation of the engine performance expressed in the throttle function. There are various options to deal with this situation (e.g., changing the mission profile itself). However, the most fruitful and elegant solution is to tweak the efficiency parameters of all the subcomponents of the engine network as it can also serve as a discussion point for hypersonic propulsion technology maturation. This combination of new efficiencies, with partial effort on the combustion process, is the minimum necessary to obtain a valid flight for this mission profile in particular, and represents the progress required for engine subsystems to allow that to happen. While a few modifications were made to the inlet and nozzle parameters, the main performance gains were attributed to the combustion process, in an effort to simulate future combustion technology enhancement, a major area

of development in hypersonic propulsion.

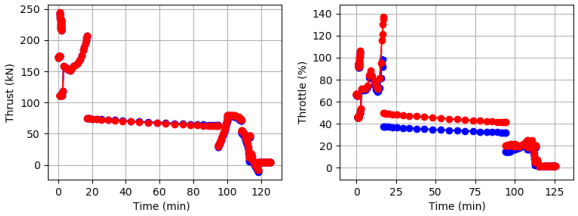

Figure 14: Comparison of the optimized solution (red) and the baseline solution (blue)

Improved efficiency leads to less fuel spent, which in turn reflects in a higher range assuming the same final fuel margin. The simulation is run again and a final range of 11,000 km is achieved.

4.2. Ascent and re-entry vehicle (HMV-ARV)

Mission profile selection For a generic hypersonic ascent and re-entry vehicle, there is a higher interest in maximizing the flight range given that the ascent phase always develops over a small time frame. In this fashion, for fixed aircraft properties (e.g., area, L/D, C_D), range may be significantly increased by achieving a higher altitude and/or speed at the end of the ascent phase since most of the flight range develops over the re-entry process. Therefore, through the built-in SUAVE optimization functions, it is possible to plot the range for an input array of initial re-entry altitude and speed, (h, v). For the purpose of this test case, the re-entry segment takes place immediately after the completion of the orbital ascent segment and, therefore, these input conditions are simultaneously the final climb altitude and speed, respectively.

To simulate the re-entry segment, estimates for L/D and C_D have to be provided. These were either based on the IXV or the Space Shuttle orbiter references [21].

Unlike the HMV-CAV cruise design trade-off, there is no point in using a similar utility function because the ascent to orbit develops over a relatively small period of time when compared to the total flight duration; on the other hand, any additional seconds during the final ascent may lead to considerable changes to the final aircraft range, as seen in Figure 15. Therefore, only the range is used as a selection criteria. The climb parameters used for the HMV-ARV are the same that have been selected for the HMV-CAV, including constant dynamic pressure for the air-breathing climb segment. The final climb design point has a final orbital speed of 6.0 km/s at an altitude of 100 km.

Baseline solution The final mission profile is represented in Figure 16. Most of the climb segments are the same as that of the HMV-CAV except for the final ascent to orbit; since no gravity turn segment exists in SUAVE, this is replaced by a linear climb at linear Mach numbers.

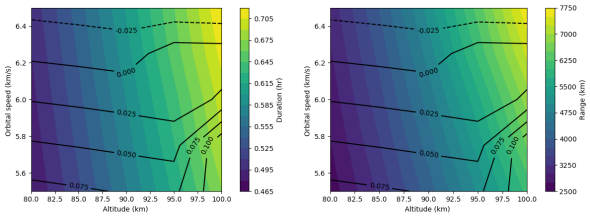

Figure 15: Range and duration for the HMV-ARV. Contour lines represent fuel margin

Weight distribution is shown in Figure 17. For the most part, fuel consumption is moderate, in line with the HMV-CAV case, until rocket operation kicks in; now the propellant consumption is rapidly increasing as both on-board oxidizer and fuel are being used. The main concern from the HMV-CAV base solution is replicated: the engine is poorly sized for the mission profile and throttle overshoots by 50%. This calls for an enhanced solution.

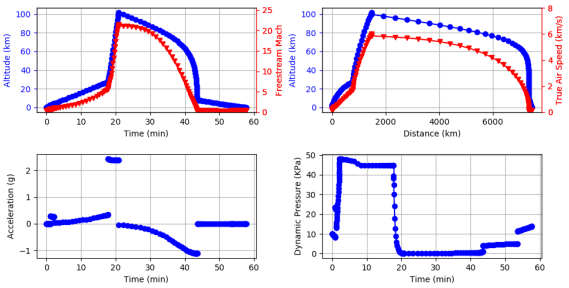

Figure 16: HMV-ARV mission profile

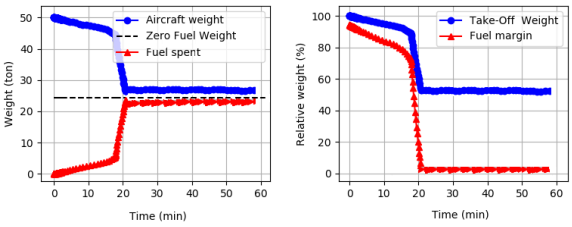

Figure 17: HMV-ARV weight distribution

Enhanced solution For the enhanced solution, the same logic from the HMV-CAV optimization case applies; that is, the burner parameters were improved to obtain a more efficient combustion. In this way, it may be possible to properly size the engine and correct the throttle issue from the pre-

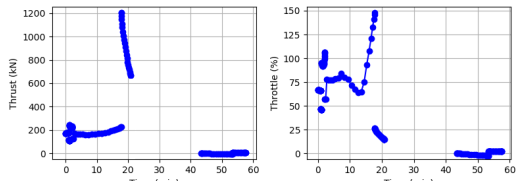

Figure 18: HMV-ARV propulsion general parameters

vious subsection. Through fuel savings it may also be possible to reach higher speeds and significantly increase the spacecraft range. For the common air-breathing cycle, the improvements are exactly the same presented for the HMV-CAV test case; rocket parameters remain unaltered. Rockets are extraordinarily sensible to weight and therefore any fuel savings are predicted to have a significant impact in the spacecraft performance. Upon improving the individual component efficiencies, the new climb design conditions are set for a final climb speed of 7.5 km/s at an altitude of 100 km.

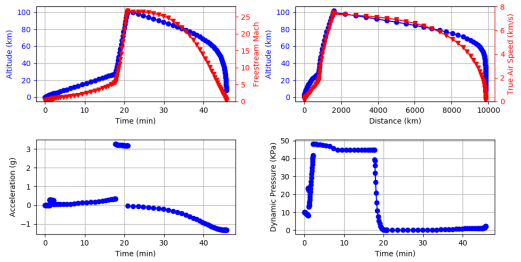

Figure 19: HMV-ARV optimized mission profile

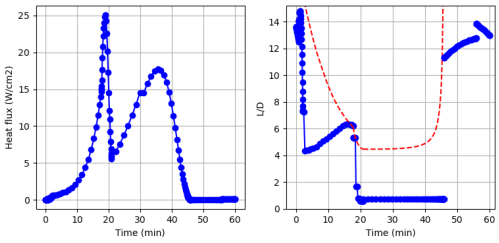

Figure 20: HMV-ARV optimized aerothermodynamic and aerodynamic distribution

5. Conclusions

The technology roadmap proved most useful in identifying and assessing various technological solutions in a multitude of technological areas: propulsion, aerodynamics, materials, thermal protection systems and control. To better understand if and how these new technologies may be incorporated in the future, a brief explanation for each one was

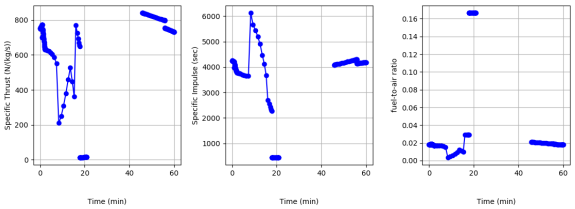

Figure 21: HMV-ARV optimized propulsion specific parameters

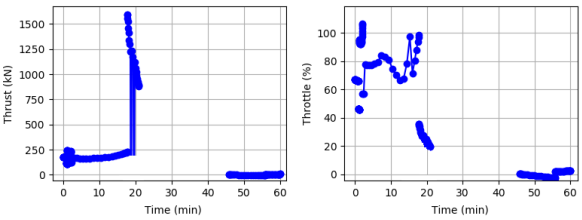

Figure 22: HMV-ARV optimized propulsion general parameters

presented and used to discuss their application in a variety of hypersonic aircraft.

Regarding the SUAVE simulations, for the same fuel margin, any of the HMV-CAV simulations outclass their respective HMV-ARV counterpart when looking at range over duration; the range for the HMV-ARV is slightly shorter but time savings can go up as much as half the airbreathing cruise scenario. This is consistent with SpaceX's predictions for sub-orbital flight when applied to Earth-to-Earth transport, which is one of the first applications for its future BFR rocket [18]. However, one of the many issues of this concept is not only the safety concerns and lack of legislation for commercial activities, but also the extreme aerothermodynamic environment these vehicles endure. The heat load is considerably shorter but that is mainly because travel time has been almost cut down in half. Heat fluxes at the nose stagnation point can go as high as 173% that of the HMV-CAV, due to the extreme speeds during the final ascent. This corroborates the need for high-performance materials and TPS for the ARV scenario and justifies the current focus on UHTC and other technologies presented throughout the roadmap development.

SUAVE is now able to run a very preliminary analysis, which can improved upon by updating the new models that have just been introduced. For instance, the scramjet model may be improved to include an isolator to simulate shock trains and chemical equilibrium equations may also be added to more accurately predict the combustion temperatures. On the other hand, the rocket model can be further expanded to include other propellant

combinations, using the Braeuning references. The aerothermodynamic model can also be be improved to give out more accurate predictions of heat distribution.

Acknowledgements
The author would like to acknowledge the help provided by the SUAVE Development Team over the SUAVE forums for their helpful insight on the SUAVE methodology and assistance with multiple Python and algorithm-related issues. The author would also like to acknowledge the support of EMBRAER for providing an extensive bibliography and guidance throughout the development of this paper.

IPFN activities received financial support from Fundação para a Ciência e Tecnologia through project UID/FIS/50010/2013

References

[1] ISO 16290:2013: Space systems Definition of the Technology Readiness Levels (TRLs) and their criteria of assessment. Standard, International Organization for Standardization, 2013.

[2] Technology Roadmaps - What Value for PSMC? Technical report, Defense Logistics Agency, 2013.

[3] Largest spacecraft to orbit and land unmanned. Technical report, Guiness World Records, 2018 (Retrieved April 23, 2018).

[4] Aerospaceweb.org. *Hypersonic Vehicle Design*, 2012 (Retrieved February 10, 2018).

[5] P. Blau. *IXV - Intermediate Experimental Vehicled*, 2015 (Retrieved April 8, 2018).

[6] R. A. Braeunig. *Liquid Oxygen and Liquid Hydrogen*, 2009 (Retrieved January 5, 2018).

[7] C. Rothmund (SNECMA). Liquid Rocket Propulsion. Presentation, Università di Roma, 2011.

[8] N. S. Chauhan and V. K. Singh. Fundamentals and Use of Hydrogen as a Fuel. *ISST Journal of Mechanical Engineering*, 6(1):63–68, 2015.

[9] Delft University. *Ideal Rocket Theory (part 1)*, Retrieved February 19, 2018).

[10] Encyclopedia Astronautica. *LE-7A*, 2002 (Retrieved May 10, 2018).

[11] Encyclopedia Astronautica. *RD-0120*, 2007 (Retrieved May 10, 2018).

[12] G. J. Harloff and B. M. Berkowitz. Hypersonic aerospace sizing analysis for the preliminary design of aerospace vehicles. *Journal of Aircraft*, 27(2):97–98, 1990.

[13] P. Hays. *How The Ramjet Engine Works*, 2017 (Retrieved October 21, 2017).

[14] W. H. Heiser and D. T. Pratt. *Hypersonic Air-Breathing Propulsion*. American Institute of Aeronautics and Astronautics, Inc.,, 1994.

[15] E. T. J.D. Harrington, Jan Wittry. *NASA Wind Tunnel Tests Lockheed Martins X-Plane Design for a Quieter Supersonic Jet*, 2017 (Retrieved March 5, 2018).

[16] John D. Anderson. *Hypersonic and High Temperature Gas Dynamics*. American Institute of Aeronautics and Astronautics (AIAA), Reston, Virginia, US, 2006.

[17] D. Kwon. The Space Shuttle Thermal Protection System. - class notes, Massachusetts Institute of Technology 2005.

[18] T. Malik. *Elon Musk Says SpaceX's Giant Mars Rocket Could Fly Passengers Around Earth*. Space.com, 2017 (Retrieved May 10, 2018).

[19] I. K. Pate. Presentation on Scramjet Engines. Presentation, University Gurgaon, 2015.

[20] M. Pouliquen. Systemes propulsifs a propergols liquides. Technical report, SNECMA, 1999-200.

[21] D. F. G. Rault. Aerodynamics of the Shuttle Orbiter at High Altitudes. *Journal of Spacecraft and Rockets*, 31(6), 1994.

[22] J. L. Ross. A fuel data standardization study for JP-4, JP-5, JP-7 and RJ-5 combusted in air. Technical report, Air Force Aero Propulsion Laboratory, Wright-Patterson Air Force Base, Ohio, 1974.

[23] United Launch Alliance (ULA). *Delta IV Launch Services Users Guide*, 2014 (Retrieved May 10, 2018).